A.K. Naveena* and N.K. Narayanan

Improving Image Search through MKFCM Clustering Strategy-Based Re-ranking Measure

https://doi.org/10.1515/jisys-2017-0227 Received May 17, 2017; previously published online April 14, 2018.

Abstract: The main intention of this research is to develop a novel ranking measure for content-based image retrieval system. Owing to the achievement of data retrieval, most commercial search engines still utilize a text-based search approach for image search by utilizing encompassing textual information. As the text information is, in some cases, noisy and even inaccessible, the drawback of such a recovery strategy is to the extent that it cannot depict the contents of images precisely, subsequently hampering the execution of image search. In order to improve the performance of image search, we propose in this work a novel algorithm for improving image search through a multi-kernel fuzzy c-means (MKFCM) algorithm. In the initial step of our method, images are retrieved using four-level discrete wavelet transform-based features and the MKFCM clustering algorithm. Next, the retrieved images are analyzed using fuzzy c-means clustering methods, and the rank of the results is adjusted according to the distance of a cluster from a query. To improve the ranking performance, we combine the retrieved result and ranking result. At last, we obtain the ranked retrieved images. In addition, we analyze the effects of different clustering methods. The effectiveness of the proposed methodology is analyzed with the help of precision, recall, and F-measures.

Keywords: Content-based image retrieval, re-ranking, image retrieval, MKFCM, four-level DWT, query image.

1 Introduction

The explosive increase in the number of photographs confronted by image search engines, for example Flickr, Google, and Yahoo, has prompted the need for an exact image retrieval framework. Inspired by effective accomplishments on the content hunt, most search engines expand upon keyword-based inquiry systems with printed data [12, 24]. Because of the way that online image search engines are oblivious to the genuine substance of images, the aftereffect of questioning for a particular picture is frequently jumbled with irrelevant data. Then again, much research has been done on content-based image retrieval (CBIR). Nevertheless, most CBIR frameworks require a client to give at least one query image [1]. In addition, image ranking as a compelling approach to enhance the results of web-based image search has been embraced by current commercial search engines. Given a query keyword, a pool of images are re-positioned by the search engines based on the query [9]. Web-scale image search engines, for the most part, utilize catchphrases as questions and depend on encompassing content to pursue images. It is outstanding that they experience the ill effects of the vagueness of question keywords. With a specific end goal of supporting the execution of web image search and overcoming the semantic gap between content data and image content, image look re-positioning, which alters the underlying positioning requests by mining visual substance or utilizing some assistant information, has been the focus of consideration as of late [13]. There are two essential methodologies in this course: visual pattern mining [6, 28] and multi-methodology fusion [26, 31].

^{*}Corresponding author: A.K. Naveena, Department of Computer Science and Engineering, College of Engineering Trikaripur, Trikaripur, India, e-mail: naveenaak@gmail.com

N.K. Narayanan: College of Engineering Vadakara, Vadakara, India

Image re-ranking means given a query keyword contribution by a client, as per a stored word-image list record, a pool of images pertinent to the inquiry catchphrase are recovered by the web index. By requesting that a client selects a query image, which mirrors the client's hunt goal, from the pool, the rest of the images in the pool are re-positioned in view of their visual similarity with the inquiry image. The visual components of images are pre-registered disconnected and stored by the search engine. The primary online computational cost of image re-positioning is on looking at visual elements. Keeping in mind the end goal to accomplish high productivity, the visual element vectors should be short and their coordination should be quick [25]. The key part of image re-positioning is to register the visual likeness between images. In distinctive inquiry images, low-level visual elements that are successful for one image classification may not function admirably for another. Many endeavors have been made in the examination of visual hunt re-positioning procedures, chiefly including characterization-based [11], grouping-based [5, 27], chart-based [6, 21, 29], and figuring-out-how-to-rank-based [10, 26] methodologies. In these techniques, visual elements assume a basic part. Be that as it may, the high dimensionality of visual components, for the most part, ranges from hundreds to thousands, which corrupts the execution of many machine learning calculations.

The query-particular visual semantic spaces can all the more precisely model the images to be re-positioned, as they have expelled other conceivably boundless numbers of non-pertinent ideas, which serve as decay of the execution of re-positioning as far as both exactness and computational cost. The visual components of images are then anticipated into their related visual semantic spaces to obtain semantic marks. At the online stage, images are re-positioned by looking at their semantic marks acquired from the visual semantic space of the query catchphrase. In addition, click-through information can be utilized to enhance the execution of image search re-positioning utilizing a singular methodology [30]. Pseudo-relevance feedback [28] is one of the strategies to utilize the re-positioning framework in the CBIR framework. Pseudo-relevance feedback utilizes all query images as positive information and treats base-positioned images of the underlying positioned list as negative information. Besides, click-based relevance feedback (CBRF) not only use navigation information to help decide the client goal, but also additionally coordinates a numerous bit learning calculation to take in the query subordinate combination weights of various modalities. CBRF influences clicked images as positive information and arbitrarily chooses images from different queries as negative information [33].

The main aim of the paper is to retrieve query-based corresponding images and to rank the images using a cluster-based similarity measure. Our proposed method has three contributions: the first one is image retrieval, the second one is ranking using clustering, and the final one is re-ranking. The method improves the ranking performance compared with the initial ranking. First, we retrieve images using a normal image retrieval method. Then, we analyze the retrieved images by utilizing fuzzy c-means (FCM) clustering, and then we re-rank the outcomes according to the distance of a cluster from a query. In experiments, we demonstrate that our technique can essentially enhance retrieval effectiveness in CBIR frameworks. The remainder of the paper is arranged as follows: Section 2 offers details about associated papers and discussion. Section 3 shows the proposed re-ranking methodology, and the experimental results are discussed in Section 4. The conclusion part is shown in Section 5.

2 Literature Survey

For the image re-ranking framework, distinctive specialists have proposed many methodologies for anomalous detection. Among them, a handful of large inquires are exhibited in this fragment. Zhang et al. [33] have explained image search re-ranking with query-dependent CBRF. Their objective was to boost content-based image indexed lists by means of image re-ranking. There were assorted modalities (components) of images that were used for re-positioning; in any case, the impacts of various modalities are queried subordinate. This algorithm stresses the fruitful utilization of navigating information for distinguishing client look expectation while utilizing multiple kernel learning algorithms to adaptively take in the question subordinate

combination weights for different modalities. They investigate a certifiable informational index gathered from a business search engine with navigating information. Moreover, Jing et al. [8] have explained a promising procedure to refine content-based image search results with visual data. Dimensionality decrease was one of the key pre-processing ventures to overcome the "scourge of dimensionality" brought by the highdimensional visual components. Here, the authors presented a dimensionality reduction algorithm called relevant local discriminant analysis (RELDA) for visual search re-ranking. As a semi-administered blend of enhanced linear discriminant analysis and locality preserving projections, the RELDA algorithm protects the nearby complex structure of the entire information and controls the pertinence between named cases. In addition, the RELDA algorithm is an explanatory type of an internationally ideal arrangement, and it was processed in view of even decay.

Furthermore, Pedronette et al. [14] have clarified the scalable re-ranking technique for CBIR. The re-ranking strategies were disclosed to use the relevant data and henceforth enhance the viability of CBIR frameworks. Other than viability, the value of those frameworks in true applications additionally relies upon the productivity and versatility of the recovery procedure, forcing an incredible test to the re-ranking methodologies, once they, for the most part, require the algorithm of separations among every one of the pictures of a given gathering. Here, they depend on the likeness of top-k records created by effective ordering structures, rather than utilizing separation data from the whole accumulation. Broad investigations were directed on an expansive image gathering, utilizing a few ordering structures. Comes about because of a thorough trial convention demonstrate that their technique acquired critical viability improvement and, in the meantime, impressively enhanced productivity. In Ref. [32], Zhang et al. have explained visual search re-ranking through Adaptive Particle Swarm Optimization (APSO). This approach consolidated the visual consistency regularization and the ranking distance of text-based ranked list. Moreover, the parameters in APSO were self-tuned adaptively, as indicated by the wellness estimations of the particles to abstain from being caught in neighborhood optima. The classification of humanoid locomotion is a troublesome exercise because of the non-linearity associated with gait signals. To select the optimal feature is a difficult task. Therefore, Semwal et al. [17] have explained a feature selection technique based on incremental feature analysis for biometric gait data classification. Moreover, Semwal et al. [16] have explained a robust and accurate feature selection for humanoid push recovery and classification: the deep learning approach. Here, the first classifier was based on the artificial neural network on the feed-forward back-propagation neural network, and the second one was based on DNN.

Additionally, Duan et al. [4] have clarified the efficient re-ranking of images from the web by utilizing the bag-based method. An image retrieval framework was a PC framework for perusing, looking for, and retrieving images from an expansive database of advanced pictures. Given a literary inquiry into customary traditional text-based image retrieval (TBIR), pertinent images were to be re-positioned utilizing visual components after the underlying content-based image look. Here, they utilized a new bag-based re-positioning system for vast-scale TBIR. They processed this issue as multiple instance learning and generalized multiple instance (GMI) learning strategy. To address the ambiguities on the occasion marks in the positive and negative packs, they proposed GMI settings. Additionally, the client log plays out the operation of individual client communication with the framework, which enhances the execution of image recovery. Similarly, Cai et al. [2] have explained attribute-assisted re-positioning for web image retrieval. Image search re-ranking was a successful way to deal with refining the content-based image item. In view of the classifiers for all the pre-characterized properties, every image was spoken to by a characteristic component comprising the reactions from these classifiers. A hypergraph was then used to show the relationship between images by incorporating low-level visual components and property highlights. Hypergraph ranking was performed to arrange the pictures. Semwal et al. [15] have explained biometric gait identification based on a multilayer perceptron. Here, they implemented a multilayered backpropagation algorithm-based artificial neural network for gait pattern classification. The kernel-based feature extraction was developed. Moreover, Singh et al. [19] have explained an information security assessment by quantifying the risk level of network vulnerabilities.

3 Proposed Re-ranking Methodology

The main aim of the proposed methodology is to develop an image re-ranking-based retrieval using the multi-kernel FCM clustering (MKFCM) algorithm. Basically, a typical CBIR framework retrieves and ranks images according to similarities based on the feature vector distance only. The idea of this model is to hybridize the results of feature-based retrieval and cluster-based retrieval. The proposed method is presented in Figure 1. Generally, the proposed retrieval model consists of two phases: (i) training and (ii) testing. In the training phase, initially, we separate the image into R, G, and B components. Then, we apply a four-level discrete wavelet transform (DWT) to each component to extract the features. After that, we apply a clustering algorithm to cluster the database images using the MKFCM algorithm. In the testing process, we calculate the features of the query image and then calculate the distance between the centroid and the query image. The

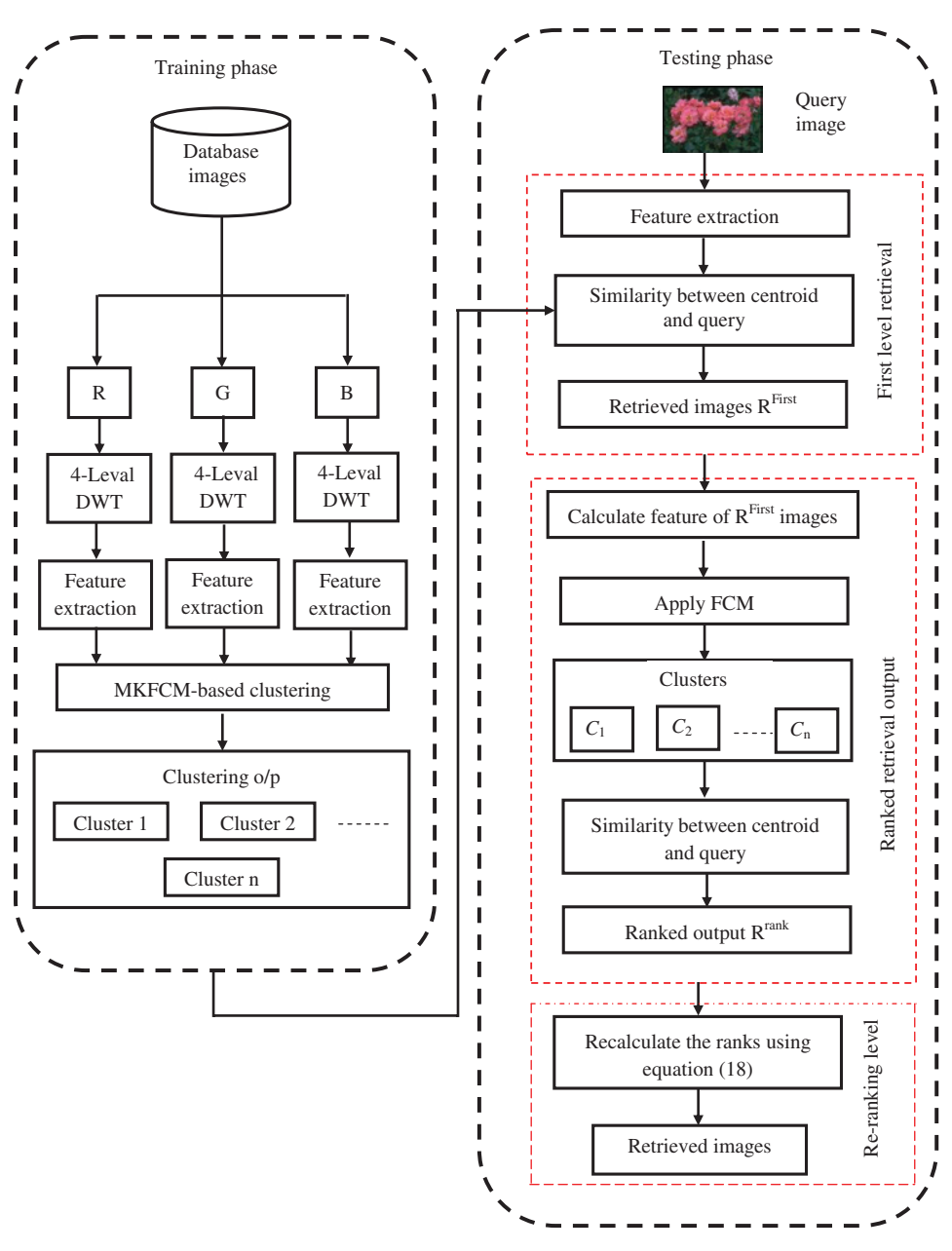


Figure 1: Overall Diagram of the Proposed Retrieval and Re-ranking Methodology.

corresponding minimum distance cluster images are retrieved. This retrieved result is considered as the firststep retrieved output. Then, the retrieved image features are calculated and we apply the FCM algorithm. After that, we calculate the difference between the centroid and the query image to rearrange clusters using the distance value. In this step, we obtain the ranked retrieval images. Finally, we combine the first-step retrieval images and the second-step ranked retrieval images to obtain the re-ranked retrieval output. The step-by-step process is explained below.

3.1 Training Phase

Consider the dataset D, which has N number of images. In this work, we used seven types of images for analysis. In the training stage, we desired to train our framework to recognize an image appropriately by its extracted feature values. Basically, the testing stage is totally dependent on the training stage. The superior training of the framework gives superior test results and better accuracy of the framework. In this proposed model, the training phase consists of three stages: (i) pre-processing, (ii) feature extraction, and (iii) clustering. The step-by-step training process is explained below.

Stage 1: Pre-processing

The fundamental target of the pre-processing stage is enhancing the image into further processing. Consider the input RGB image, and we decompose the RGB image into R, G, and B components. These components are used for further processing.

Stage 2: Feature extraction

Feature extraction is an important process of image retrieval. In this, useful features are extracted from the image for retrieval purpose. Our proposed system uses four-level DWT for image feature extraction. The DWT splits the image into high- and low-frequency components. In the first level of decomposition, there are four sub-bands obtained, such as LL1, LH1, HL1, and HH1, For each successive level of decomposition, the LL subband of the previous level is used as the input. To perform second-level decomposition, the DWT is applied to the LL1 band, which decomposes the LL1 band into four sub-bands, such as LL2, LH2, HL2, and HH2. To perform the third decomposition, the DWT is applied to the LL2 band, which decomposes this band into the four sub-bands LL3, LH3, HL3, and HH3. To perform fourth-level decomposition, the DWT is applied to the LL3 band, which decomposes this band into again four sub-bands LL4, LH4, HL4, and HH4. The fourlevel DWT decomposition is shown in Figure 2. After the four-level decomposition, we select the third- and fourth-level LL coefficient. These selected coefficients are considered as the two types of features. Then, we calculate the standard deviation (SD) of the third and fourth sub-bands of all the three components. The SD is calculated using Eq. (1). Here, we obtain the eight features of each component. Totally, we obtain 24 features for one image. Using this procedure, we calculate the features for all the images. The standard deviation is calculated using Eq. (1):

$$SD = \sqrt{\frac{1}{N} \sum_{i=1}^{N} (Y_i - \mu)^2}.$$
 (1)

$$\mu = \frac{1}{N} \sum_{i=1}^{N} Y_i. \tag{2}$$

Here, we consider that N is representing the amount of wavelet coefficient at the specific sub-band, while Y_i is the wavelet coefficient value at a specific point at that sub-band.

Stage 3: MKFCM-based clustering

After the feature extraction, we apply the clustering process to group the database images into N-number of clusters. In this paper, we used seven as the number of clusters. Here, we use MKFCM for the clustering

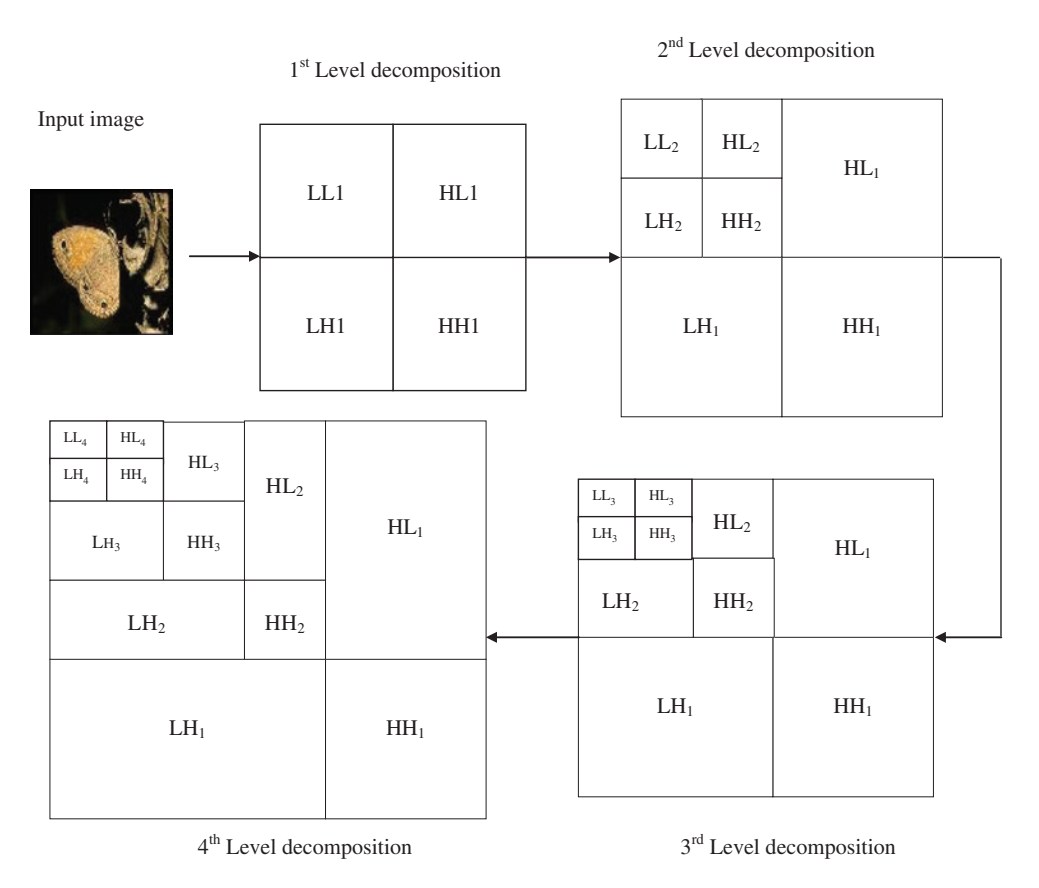


Figure 2: Four-Level Discrete Wavelet Transforms.

process. MKFCM is already used for a lot of image segmentation processes [3, 7, 22]. Huang et al. [7] proposed the multiple MKFCM algorithm, which extends the FCM algorithm with the multiple-kernel learning setting also used for face clustering. In the multi-kernel process, there are two hybrid kernels such as the linear and quadratic kernels. In hybrid work, new hybridized kernel functions are taken and the clustering process is performed based on these hybrid kernel functions. Let k_1 and k_2 be two kernels. Then, three hybrid kernels are formulated based on the definition given in Refs. [3, 18].

$$K(p, q) = K_1(p, q) + K_2(p, q)$$
 is a kernel.

$$K(p, q) = \alpha * K_1(p, q)$$
 is a kernel, when $\alpha > 0$.

$$K(p, q) = K_1(p, q) * K_2(p, q).$$

The general framework of the proposed MKFCM aims to minimize the objective function that is given in Eq. (3):

$$F = \sum_{i=1}^{N} \sum_{j=1}^{a} M_{ij}^{m} (1 - K_{MK}(t_{j}, A_{i})),$$
(3)

where *N* is the number of clusters, *a* is the number of data points, M_{ii} is the membership of j^{th} data in the i^{th} cluster A, A is the cluster center, K_{MK} is the multiple kernel function, and m is the degree of fuzziness of the algorithm.

In MKFCM, t_i represents the kernel function $K_{MK}(x, y)$. Here, we are considering that multiple kernels for our proposed work are linear and quadratic kernels.

(i) Applying the first theorem

Step 1: At first, randomly initialize the cluster size *a*.

Step 2: Randomly choose the centroid for each cluster A,

Step 3: Calculate the objective function *F*:

$$F = \sum_{i=1}^{N} \sum_{j=1}^{a} M_{ij}^{m} (1 - K_{MK}(t_{j}, A_{i})).$$

Step 4: Substitute the first theorem in Eq. (3), where K_1 is a linear kernel and K_2 is the quadratic kernel.

$$K_{MK}(p, q) = K_1(p, q) + K_2(p, q),$$
 (4)

$$K_{1}(p,q) = p^{T}q + c, (5)$$

$$K_2(p,q) = 1 - \frac{||p-q||^2}{||p-q||^2 + c},$$
 (6)

where *c* is a constant value.

Step 5: Then, we calculate the cluster center using Eq. (7):

$$A_{i} = \frac{\sum_{i=1}^{N} M_{ij}^{m} K_{MK}(p, q)}{\sum_{i=1}^{N} M_{ij}} .$$
 (7)

Step 6: Membership update is done by using Eq. (8):

$$M_{ij} = \frac{1}{\sum_{K=1}^{A} \left(\frac{\left\| K_{MK}(p, q) - A_{i} \right\|}{\left\| K_{MK}(p, q) - A_{K} \right\|} \right)^{\frac{2}{m-1}}}.$$
(8)

Based on the MKFCM, the images are clustered. In this work, we utilize the cluster size N=7.

(ii) Applying the second theorem

When applying the second theorem to the FCM, at first we randomly initialize the cluster size. After that, we calculate the kernel-based objective function *F*.

$$F = \sum_{i=1}^{N} \sum_{j=1}^{a} M_{ij}^{m} (1 - K_{MK}(t_{j}, A_{i})),$$

where

$$K_{MK} = \alpha * K_1(p, q), \tag{9}$$

where α is a random value. In this paper, we take the random value as 0.1.

$$F = \sum_{i=1}^{N} \sum_{i=1}^{a} M_{ij}^{m} (1 - \alpha * K_{1}(p, q)(t_{j}, A_{i})),$$
(10)

$$K_1(p,q) = p^T q + c, \tag{11}$$

$$A_{i} = \frac{\sum_{i=1}^{N} M_{ij}^{m} (\alpha * K_{1}(p, q))}{\sum_{i=1}^{N} M_{ij}},$$
(12)

(iii) Applying the third theorem

In this section, we explain the third theorem. Here, we use the kernel K_{MK} , which is $k_1(p,q)*k_2(p,q)$. The objective function of theorem 3 is given in Eq. (14):

$$F = \sum_{i=1}^{N} \sum_{j=1}^{a} M_{ij}^{m} (1 - (K_{1}(p, q) * K_{2}(p, q))(t_{j}, A_{i}))$$

$$K_{1}(p, q) = p^{T}q + c.$$
(14)

$$K_2(p, q) = 1 - \frac{||p-q||^2}{||p-q||^2 + c}.$$
 (15)

$$A_{i} = \frac{\sum_{i=1}^{N} M_{ij}^{m} (K_{1}(p, q) * K_{2}(p, q))}{\sum_{i=1}^{N} M_{ij}}.$$
 (16)

$$M_{ij} = \frac{1}{\sum_{K=1}^{A} \left(\left\| (K_{1}(p, q) * K_{2}(p, q)) - A_{i} \right\| \right)^{\frac{2}{m-1}}}.$$

$$(17)$$

Based on the above three theorems, in this paper, we perform the clustering process and the effectiveness of the performance of these three algorithms is analyzed in Section 4. Based on the MKFCM, the images are clustered. In this work, we utilize the cluster size N=7. After the MKFCM process, we obtain the number of cluster sets, such as C_1 , C_2 , C_3 , C_4 , C_5 , C_6 , C_7 These clustered images are used for the testing process.

3.2 Testing Phase

After the training process is completed, we start doing the testing process. The testing phase depends on the training phase only. The testing process images are fully different from the training images; however, the categories are the same. In the testing process, query-based images are retrieved using multiple stages.

Step 1: Consider the query image Q_i , which is present in database D. In this paper, at first we have given the query image to the system. The aim of this section is to retrieve the corresponding query-based images in the ranked format.

Step 2: Then, we apply four-level DWT to the image for calculating the features of the query image. The feature extraction process is explained in the training phase, and the same process is also repeated in this testing process.

Step 3: After that, we take the similarities between centroid (obtained from the training process) and query image features. The minimum distance-based corresponding cluster (C_i) images are retrieved. The retrieved images are ranked in decreasing order of similarity between the query image and cluster. This output is called first-level retrieval output R^{First} . Based on the image position, we generate the index R^{First} .

Step 4: After the first-level retrieval, we rank the images because the obtained retrieval results are not properly ranked. Therefore, in this paper, we introduce the ranking methodology. To rank the first-level retrieval result images R^{First} , we group the images using the clustering process.

Step 5: Before applying the clustering process to *R*^{First} images, we calculate the features of all the retrieved images. The features are already extracted in the training phase.

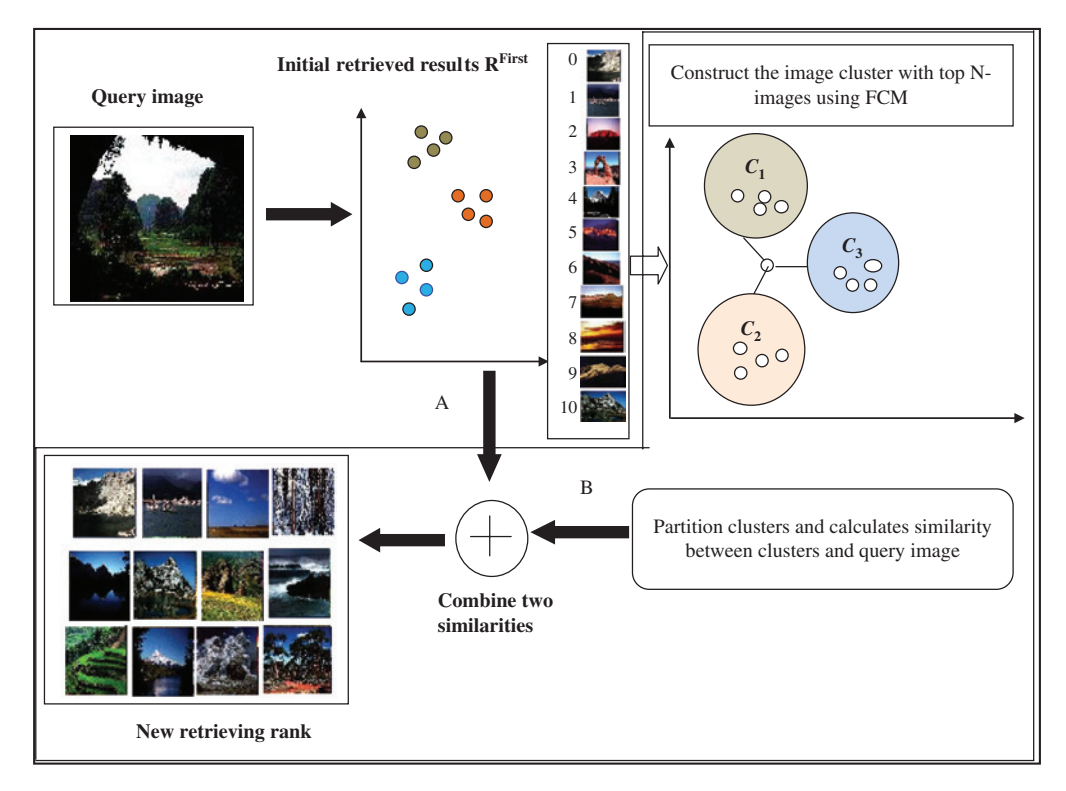


Figure 3: Re-evaluating Similarity.

Step 6: In this, we utilize the FCM clustering algorithm for clustering the image features. Here, we group the R^{First} images into N-number of clusters $(C_1, C_2, ..., C_N)$ based on a distance measure.

Step 7: Then, we calculate the similarities between centroid A, and query images. Based on the similarities, we arrange the clusters $(C_1, C_2, ..., C_N)$. The cluster-based images are retrieved. In this step, we obtain the retrieved result, called ranked retrieval result R^{Rank} . Based on the image position, we generate the index $R^{\text{Rank}}_{\text{Index}}$.

Step 8: To improve the ranking performance of images, we perform re-ranking. Here, we combine $R_{\text{index}}^{\text{First}}$ and $R_{\text{Index}}^{\text{Rank}}$ using Eq. (18):

$$D'(I, I') = R_{\text{Index}}^{\text{First}} + R_{\text{Index}}^{\text{Rank}}, \tag{18}$$

where $R_{\rm Index}^{\rm First}$ represents the first-level retrieval output index, $R_{\rm Index}^{\rm First}$ represents the ranked retrieval result index, and D'(I, I') represents the re-ranked retrieved result. Utilizing Eq. (18), we re-calculate the similarities between the query image and the images in the retrieved result. At that point, we re-arrange the positions of the images as indicated by the re-calculated values in decreasing order. Figure 3 demonstrates the arrangement of recalculating the similarity that clarifies the development of image cluster and the combination of two similarities. Here, the images that have more similarity to each other are assembled into one group and insignificant images are separated into various groups. In this way, the similarity between the query and the images in the closer group is adjusted in accordance with a smaller value; otherwise, the similarity is modified to a larger value by Eq. (18).

4 Results and Discussion

In this section, we discuss the results obtained from improving the image search through the KFCM clustering strategy-based re-ranking. This proposed technique is done in Windows machine having Intel Core i3 processor with speed 1.9 GHz and 4 GB RAM. For evaluating the performance of the proposed work, we used seven



Figure 4: Experimentally Used Sample Image.

categories of images: butterfly, nature, rose, car, deer, waterfall, and Tajmahal, which were collected from the Internet. Each image had a different quantity and a total of 700 images were used, including 100 butterfly images, 100 nature images, 100 rose images 100 car images, 100 deer images, 100 waterfall images, and 100 Tajmahal images. In this, 90% of the images were used for the training process and 10% of the images were used for the testing process. The sample experimentally used images are given in Figure 4.

4.1 Performance Measures

System performance is analyzed by using the most common performance measures, known as precision (P), recall (R), and F-measure (F). A precision rate can be defined as the percentage of retrieved images similar to the query among the total number of retrieved images. A recall rate is defined as the percentage of retrieved images that are similar to the query among the total number of images similar to the query in the database. It can be easily seen that both precision and recall rates are the functions of the total number of retrieved images. In order to have a high accuracy, the system needs to have both high precision and high recall rates. Mathematically, P, R, and F are defined as

$$P = \frac{N^Q}{T^Q} \times 100,\tag{19}$$

$$R = \frac{N^Q}{D^Q} \times 100,\tag{20}$$

$$F=2\times\frac{P\cdot R}{P+R},\tag{21}$$

where N^Q represents the number of relevant images retrieved from the database, T^Q represents the total number of images retrieved, and D^Q represents the number of images in the database relevant to query image Q.

4.2 Experimental Results in the Proposed Approach

In this section, we show the visual representation of the proposed algorithm. The visual results contain the query image, first-level retrieval output, and final re-ranked images. Figures 5–7 show the visual results of three images, such as butterfly, car, and rose.

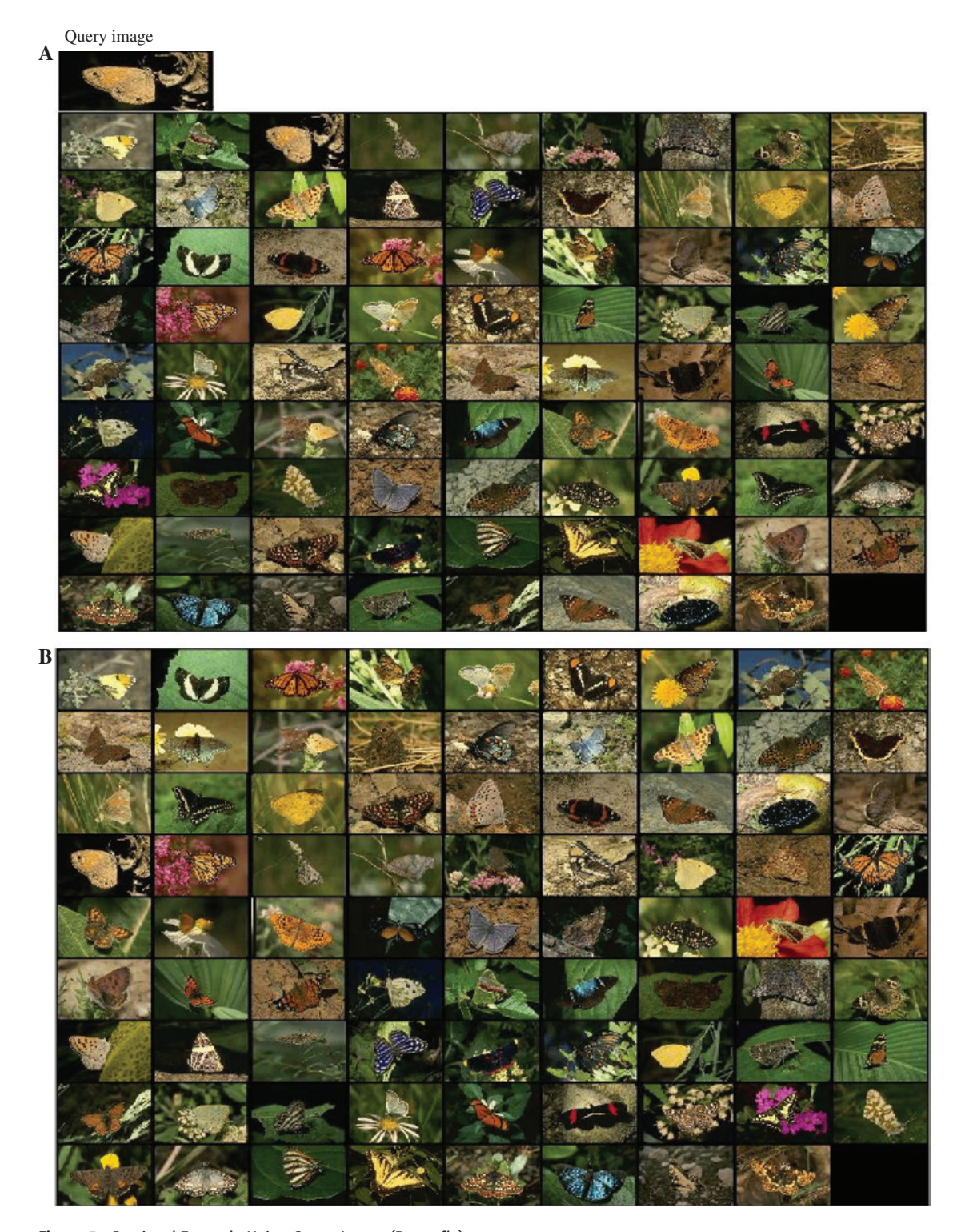


Figure 5: Retrieval Example Using Query Image (Butterfly). (A) First-level retrieval output images. (B) Re-ranked image output.

4.3 Comparative Analysis

The performance of the proposed image retrieval and re-ranking system is analyzed with the help of precision, recall, and F-measure, which are the most significant performance parameters. The effectiveness of the

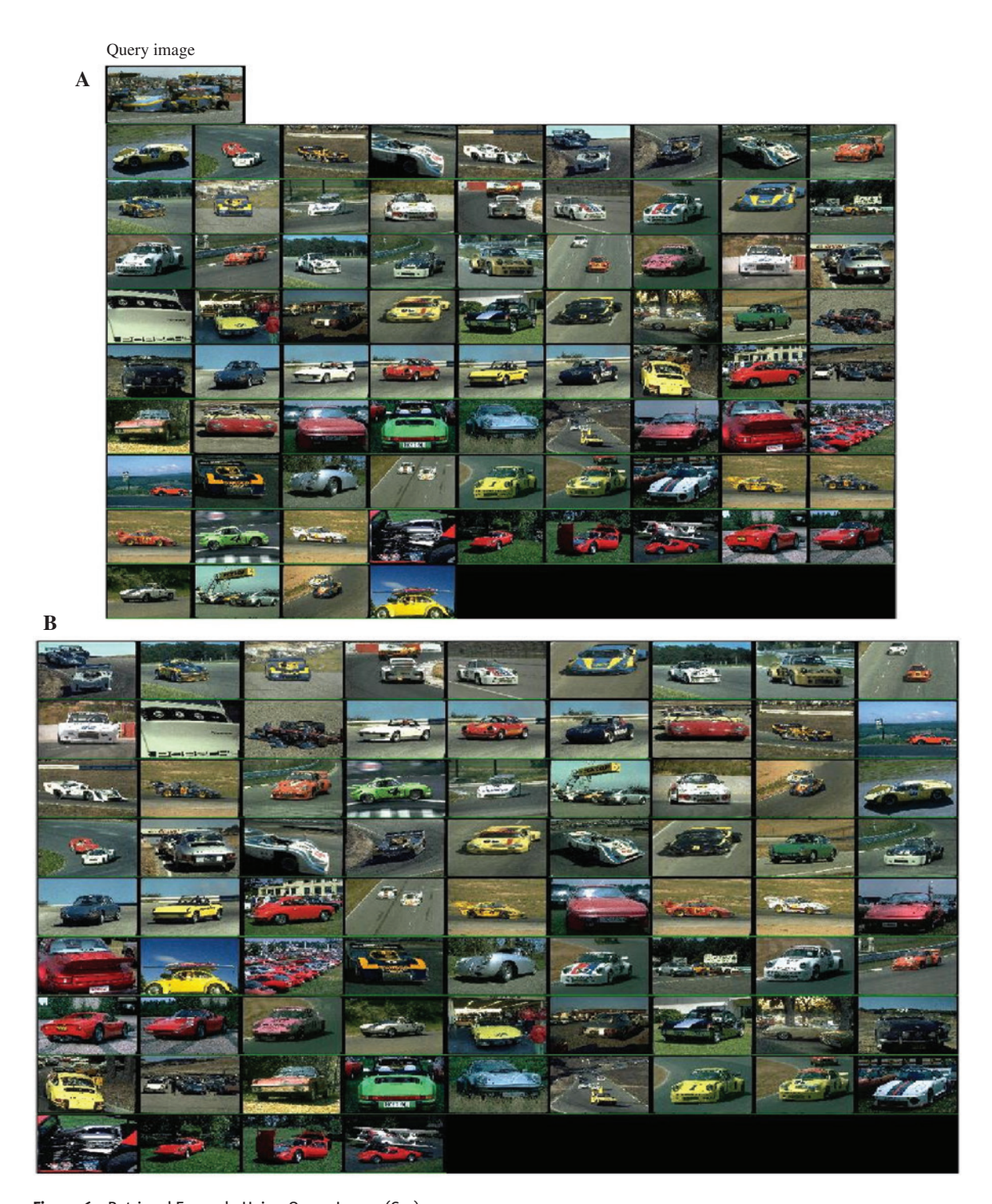


Figure 6: Retrieval Example Using Query Image (Car).
(A) First-level retrieval output images. (B) Re-ranked image output.

proposed technique is demonstrated by performing a comparison between the retrieval results of the proposed MKFCM clustering method with other approaches. The principal objective of the proposed system is to effectively rank the retrieved images. Here, at first, we convert the input image into R, G, and B components. Then, we extract the features of the three components using four-level DWT. Then, we apply the MKFCM clustering algorithm to cluster the images using distance measures. After that, the query-based image clusters are



Figure 7: Retrieval Example Using Query Image (Rose). (A) First-level retrieval output images. (B) Re-ranked image output.

retrieved. Then, we rank the retrieved images using the FCM algorithm. To improve the efficiency of ranking performance, in this paper we propose a re-ranking method. Here, we prove the effectiveness of the proposed approach and compare our work with the different theorems.

Figures 8–10 analyze the performance of the proposed approach using different measures. In this work, for the training process, we utilized the MKFCM algorithm. In multi-kernels, we used linear and quadratic kernels. Based on the hybrid kernels, we implemented three theorems. Based on the three kernels, we evaluated the results. Figure 8 shows the performance analysis of different approaches using the precision value. Here, the *x*-axis represents the query images and the *y*-axis represents the precision value. When the query image is "butterfly", we obtain the maximum precision of 0.8 for using theorem 1, 0.6 for using theorem 2, 0.76 for using theorem 3, and 0.4 for using k-means algorithm-based re-ranking. When analyzing Figure 8, we obtain the maximum precision of 0.83 for the rose image using theorem 1. Comparing these four methods,

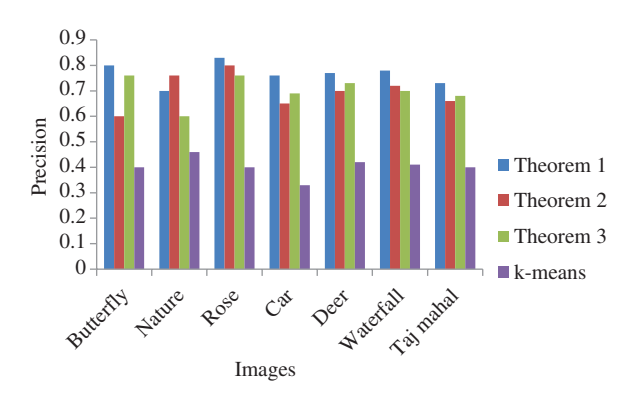


Figure 8: Performance Analysis of Different Approaches Using Precision Measure.

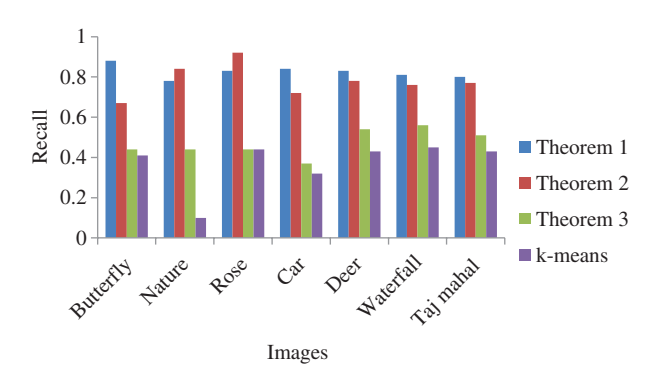


Figure 9: Performance Analysis of Different Approaches Using Recall Measure.

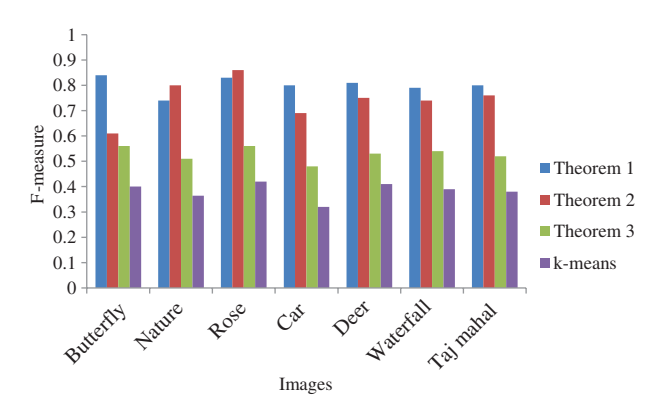


Figure 10: Performance Analysis of Different Approaches Using F-measure.

theorem 1 obtains the better result compared to theorem 2, theorem 3, and the k-means algorithm. Similarly, the k-means algorithm-based image re-ranking method has poor performance compared to the other three methods. Figure 9 shows the performance analysis of different approaches using recall measure. Using theorem 1, we obtain the maximum recall of 0.88 for the butterfly image; using theorem 2, we obtain the maximum recall of 0.92 for the rose image; using theorem 3, we obtain the maximum recall of 0.56 for the waterfall image; and using the k-means algorithm, we obtain the maximum recall of 0.45 for the waterfall image. Moreover, Figure 10 shows the performance analysis of a different approach using F-measure. From the result, we clearly understand that our proposed approach obtains the better performance.

Tables 1–4 show the confusion matrix of theorem 1, theorem 2, theorem 3, and k-means-based retrieval. Here, the user gives the query to the system and the query-based images are retrieved. In the confusion matrix, this is the diagonal element divided by the sum over the relevant row. Table 1 shows the confusion matrix of theorem 1. Here, the user-recommended number of images is 100. So, when we give the query image, the query-based 100 images are retrieved. It is equivalent to recall. Using theorem 1, we obtain 80 butterfly images, six nature images, three rose images, one car image, four deer images, three waterfall images, and four Tajmahal images for "butterfly image". We correctly retrieve 80%. Compared to the entire confusion matrix, we obtain the maximum retrieval accuracy for theorem 1, theorem 2, and theorem 3. The best average

Table 1: Confusion Matrix for Theorem 1.

	Butterfly	Nature	Rose	Car	Deer	Waterfall	Tajmahal
Butterfly	80 (80%)	6 (6%)	3 (3%)	1 (1%)	4 (4%)	3 (35)	4 (4%)
Nature	10 (10%)	70 (70%)	6 (6%)	4 (4%)	3 (3%)	4 (4%)	4 (4%)
Rose	4 (4%)	3 (5%)	83 (83%)	3 (5%)	2 (2%)	3 (2%)	2 (2%)
Car	8 (8.8%)	4 (4%)	4 (4%)	76 (76%)	3 (3%)	4 (4%)	2 (2%)
Deer	6 (6.6%)	3 (3.3%)	1 (1.1%)	4 (4%)	77 (77%)	5 (5%)	5 (5%)
Waterfall	3 (5%)	2 (2%)	3 (2%)	2 (2%)	6 (6%)	78 (78%)	6 (6%)
Tajmahal	5 (5%)	6 (6%)	3 (3.3%)	5 (5%)	2 (2%)	6 (6%)	73 (73%)

Table 2: Confusion Matrix for Theorem 2.

	Butterfly	Nature	Rose	Car	Deer	Waterfall	Tajmahal
Butterfly	60 (60%)	10 (10%)	4 (4%)	3 (35)	4 (4%)	13 (13%)	7 (7%)
Nature	4 (4%)	76 (76%)	5 (5%)	5 (5%)	4 (4%)	3 (35)	4 (4%)
Rose	3 (3%)	4 (4%)	81 (81%)	4 (4%)	4 (4%)	3 (3%)	2 (2%)
Car	3 (3%)	4 (4%)	11 (11%)	65 (65%)	3 (3%)	4 (4%)	11 (11%)
Deer	6 (11%)	5 (5%)	2 (2%)	2 (2%)	74 (74%)	6 (6%)	5 (5%)
Waterfall	6 (6%)	4 (4%)	5 (5%)	6 (6%)	5 (5%)	70 (70%)	4 (4%)
Tajmahal	5 (5%)	3 (3%)	6 (6%)	4 (4%)	5 (5%)	5 (5%)	72 (72%)

Table 3: Confusion Matrix for Theorem 3.

	Butterfly	Nature	Rose	Car	Deer	Waterfall	Tajmahal
Butterfly	40 (40%)	11 (11%)	6 (6%)	7 (7%)	7 (7%)	20 (20%)	10 (10%)
Nature	7 (7%)	40 (40%)	20 (20%)	10 (10%)	11 (11%)	6 (6%)	7 (7%)
Rose	15 (15%)	10 (10%)	40 (40%)	25 (25%)	4 (4%)	4 (4%)	3 (3%)
Car	15 (15%)	20 (20%)	7 (7%)	33 (33%)	10 (10%)	10 (10%)	5 (5%)
Deer	15 (15%)	10 (10%)	11 (11%)	10 (10%)	36 (36%)	11 (11%)	7 (7%)
Waterfall	11 (11%)	10 (10%)	9 (9%)	15 (15%)	10 (10%)	40 (40%)	5 (5%)
Tajmahal	12 (12%)	10 (10%)	11 (11%)	9 (9%)	6 (6%)	4 (4%)	38 (38%)

Table 4: Confusion Matrix for k-Means Clustering.

	Butterfly	Nature	Rose	Car	Deer	Waterfall	Tajmahal
Butterfly	37 (37%)	4 (4%)	10 (10%)	9 (9%)	7 (7%)	20 (20%)	14 (14%)
Nature	10 (10%)	20 (20%)	19 (19%)	10 (10%)	11 (11%)	15 (15%)	15 (15%)
Rose	22 (24.4%)	19 (21.1%)	25 (44.4%)	20 (22.2%)	12 (12%)	6 (6%)	6 (6%)
Car	20 (20%)	11 (11%)	20 (20%)	28 (28%)	7 (7%)	8 (8%)	6 (6%)
Deer	11 (11%)	13 (13%)	15 (15%)	11 (11%)	35 (35%)	9 (9%)	6 (6%)
Waterfall	13 (13%)	10 (10%)	11 (11%)	9 (9%)	15 (15%)	32 (32%)	15 (15%)
Tajmahal	10 (10%)	9 (9%)	11 (11%)	15 (15%)	10 (10%)	15 (15%)	30 (30%)

Table 5: Comparative Analysis Based on Average Precision Measure.

	Butterfly	Nature	Rose	Car	Deer	Waterfall	Tajmahal
Theorem 1	0.8	0.7	0.83	0.76	0.77	0.78	0.73
Theorem 2	0.6	0.76	0.8	0.65	0.7	0.72	0.68
Theorem 3	0.76	0.6	0.76	0.69	0.73	0.7	0.67
Voravuthikunchai et al. [23]	0.59	0.64	0.69	0.65	0.68	0.66	0.65
Srilatha [20]	0.6	0.65	0.7	0.66	0.67	0.67	0.64

precision of 83%, 80%, 76%, and 46% was obtained using theorem 1, theorem 2, theorem 3, and k-means, respectively. To evaluate the significance of the obtained results, we employed the analysis of variance test on the maximum precision values. We ranked all models by maximum precision and evaluated groups of models to find classes with similar intra-class performance and significantly different inter-class performance. From Section 4, we clearly understand that our proposed approach is better than k-means algorithm-based retrieval.

4.4 Comparative Analysis of Other Works

Here, we compare our proposed work with other published works related to image retrievals, such as those of Voravuthikunchai et al. [23] and Srilatha [20]. In Ref. [23], the authors explained an image re-ranking based on statistical f frequency patterns. More specifically, the approach consists in computing efficiently and onthe-fly frequent closed patterns, and in re-ranking images based on the number of patterns they contain. Similarly, in Ref. [20], the authors explained a scalable image search re-ranking through the CBIR method. Here, k-means clustering, support vector machine classifier, and re-ranking algorithm technique are used to obtain the efficient prototype-based scalable result.

Table 5 shows the comparative analysis based on precision measures. Here, we compare our proposed three theorems with existing two approaches. Our proposed approach achieves the maximum precision of 0.83 for theorem 1 using a rose image, which is 0.69 for using Ref. [23] and 0.7 for using Ref. [20]. From the result, we clearly understand that our proposed approach achieves the maximum output compared to other works.

5 Conclusion

In this paper, an MKFCM technique has been projected and applied as the general framework for image retrieval and re-ranking problems, where the kernel function is composed by multiple kernels. Here, we implemented three theorems based on kernels. The projected method first retrieves the corresponding image, then ranks the image, and finally re-ranks the image. The first-level retrieval, ranking, and re-ranking methods were analyzed. The performance of the image retrieval was assessed using precision, recall, and

F-measure. From the experimental results, we conclude that our proposed approach is better than the other approaches based on precision, recall, and F-measure. We believe that our proposed system can serve as a practical tool for online applications. In the future, we plan to develop new re-ranking algorithms, with the inclusion of optimization with the conventional feature extraction scheme to improve the retrieval accuracy.

Bibliography

- [1] N. Ben-Haim, B. Babenko and S. Belongie, Improving web-based image search via content based clustering, in: Computer Vision and Pattern Recognition Workshop, 2006.
- [2] J. Cai, Z. Zha, W. Zhou and Q. Tian, Attribute-assisted reranking for web image retrieval, in: Proceedings of the 20th ACM international conference on Multimedia, pp. 873-876, 2012.
- [3] L. Chen, C. L. P. Chen and M. Lu, A multiple-kernel fuzzy C-means algorithm for image segmentation, IEEE Trans. Syst. Man Cybernet. Part B (Cybernet.) 41 (2011), 1263-1274.
- [4] L. Duan, W. Li, I. W. -H. Tsang and D. Xu, Improving web image search by bag-based reranking, IEEE Trans. Image Process. 20 (2011), 3280-3290.
- [5] W. Hsu, L. Kennedy and S. Chang, Video search re-ranking via information bottle-neck principle, in: Proceedings of the 14th Annual ACM International Conference on Multimedia, pp. 35-44, 2006.
- [6] W. H. Hsu, L. S. Kennedy and S. F. Chang, Video search re-ranking through random walk over document-level context graph, in: Proc. 15th International Conference Multimedia, pp. 971–980, 2007.
- [7] H.-C. Huang, Y.-Y. Chuang and C.-S. Chen, Multiple kernel fuzzy clustering, IEEE Trans. Fuzzy Syst. 20 (2012), 120-134.
- [8] P. Jing, Z. Ji, Y. Yu and Z. Zhang, Visual search re-ranking with relevant local discriminant analysis, Neurocomputing 173 (2016), 172-180.
- [9] S. Keerthana, R. C. Narayanan and K. Krishnamoorthy, Efficient re-ranking of images from the web using bag based method, Int. J. Comput. Appl. 42 (2012).
- [10] Y. Liu and T. Mei, Optimizing visual search re-ranking via pair wise learning, IEEE Trans. Multimed. 13 (2011), 280-291.
- [11] Y. Liu, T. Mei, X. Hua, J. Tang, X. Wu and S. Li, Learning to video search re-rank via pseudo preference feedback, in: Proceedings of the IEEE International Conference on Multimedia and Expo, pp. 207-210, 2008.
- [12] Y. Liu, T. Mei and X. S. Hua, Crowd re-ranking: exploring multiple search engines for visual search re-ranking, in: ACM SIGIR, pp. 500-507, 2009.
- [13] T. Mei, Y. Rui, S. Li and Q. Tian, Multimedia search re-ranking: a literature survey, ACM Comput. Surv. 46 (2014), 38.
- [14] D. C. G. Pedronette, J. Almeida and R. d. S. Torres, A scalable re-ranking method for content-based image retrieval, Inform. Sci. 265 (2014), 91-104.
- [15] V. B. Semwal, M. Raj and G. C. Nandi, Biometric gait identification based on a multilayer perceptron, Robot. Autonom. Syst. **65** (2015), 65–75.
- [16] V. B. Semwal, K. Mondal and G. C. Nandi, Robust and accurate feature selection for humanoid push recovery and classification: deep learning approach, Neural Comput. Appl. 28 (2017), 565-574.
- [17] V. B. Semwal, J. Singha, P. K. Sharma, A. Chauhan and B. Behera, An optimized feature selection technique based on incremental feature analysis for bio-metric gait data classification, Multimed. Tools Appl. 76 (2017), 24457-24475.
- [18] J. Shawe-Taylor and N. Cristianini, Kernel Methods for Pattern Analysis, Cambridge University Press, Cambridge, UK, 2004.
- [19] U. K. Singh, C. Joshi and N. Gaud, Information security assessment by quantifying risk level of network vulnerabilities, Int. J. Comput. Appl. 156 (2016), 37-44.
- [20] T. Srilatha, Scalable image search re-ranking through content based image retrieval (CBIR) method, Int. J. Adv. Res. Comput. Sci. 7 (2016).
- [21] X. Tian, L. Yang, J. Wang, Y. Yang, X. Wu and X. Hua, Bayesian video search re-ranking, in: Proceedings of ACM International Conference on Multimedia, pp. 131-140, 2008.
- [22] N. Venu and B. Anuradha, Two different multi-kernels for fuzzy C-means algorithm for medical image segmentation, Int. J. Eng. Trends Technol. (IJETT) 20 (2015), 77-82.
- [23] W. Voravuthikunchai, B. Crémilleux and F. Jurie, Image re-ranking based on statistics of frequent patterns, in: ACM, 2014.
- [24] L. Wang, L. Yang and X. Tian, Query aware visual similarity propagation for image search re-ranking, in: ACM Multi Media,
- [25] X. Wang, K. Liu and X. Tang, Query-specific visual semantic spaces for web image re-ranking, in: Computer Vision and Pattern Recognition, IEEE Conference, 2011.
- [26] M. Wang, H. Li, D. Tao, K. Lu and X. Wu, Multimodal graph-based re-ranking for web image search, IEEE Trans. Image Process. **21** (2012), 4649–4661.
- [27] S. Wei, Y. Zhao, Z. Zhu and N. Liu, Multimodal fusion for video searches re-ranking, IEEE Trans. Knowl. Data Eng. 22 (2010), 1191-1199.

- [28] R. Yan, A. Hauptmann and R. Jin, Multimedia search with pseudo relevance feedback, in: Proc. 2nd Int. CIVR, pp. 238-247,
- [29] Y. Yang, W. Hsu and H. Chen, Online re-ranking via ordinal informative concepts for context fusion in concept detection and video search, IEEE Trans. Circuits Syst. Video Technol. 19 (2009), 1880-1890.
- [30] X. Yang, Y. Zhang, T. Yao, Z. J. Zha and C. W. Ngo, Click-boosting random walk for image search re-ranking, in: Proc. 5th ICIMCS, 2013.
- [31] X. Yang, Y. Zhang, T. Yao, C. W. Ngo and T. Mei, Click-boosting multi-modality graph-based re-ranking for image search, in: Multimedia System, pp. 1-11, 2014.
- [32] L. Zhang, T. Mei, Y. Liu, D. Tao and H.-Q. Zhou, Visual search re-ranking via adaptive particle swarm optimization, Pattern Recogn. 44 (2011), 1811-1820.
- [33] Y. Zhang, X. Yang and T. Mei, Image search re-ranking with query-dependent click-based relevance feedback, IEEE Trans. Image Process. 23 (2014), 4448-4459.